Molecular Cell
Article

Replication Termination at Eukaryotic Chromosomes Is Mediated by Top2 and Occurs at Genomic Loci Containing Pausing Elements

Daniele Fachinetti,[1,2] Rodrigo Bermejo,[1,2] Andrea Cocito,[1] Simone Minardi,[3] Yuki Katou,[4] Yutaka Kanoh,[4] Katsuhiko Shirahige,[4] Anna Azvolinsky,[5] Virginia A. Zakian,[5] and Marco Foiani[1,2,*]
[1]Fondazione IFOM, Istituto FIRC di Oncologia Molecolare (IFOM-IEO Campus), Via Adamello 16, 20139, Milan, Italy
[2]DSBB-Università degli Studi di Milano, 20133 Milan, Italy
[3]COGENTECH (Consortium for Genomic Technologies), 20139 Milan, Italy
[4]Tokyo Institute of Technology, Yokohama City, 226-8501 Kanagawa, Japan
[5]Princeton University, Princeton, NJ 08544-1014, USA
*Correspondence: marco.foiani@ifom-ieo-campus.it
DOI 10.1016/j.molcel.2010.07.024

SUMMARY

Chromosome replication initiates at multiple replicons and terminates when forks converge. In *E. coli*, the Tus-*TER* complex mediates polar fork converging at the terminator region, and aberrant termination events challenge chromosome integrity and segregation. Since in eukaryotes, termination is less characterized, we used budding yeast to identify the factors assisting fork fusion at replicating chromosomes. Using genomic and mechanistic studies, we have identified and characterized 71 chromosomal termination regions (*TERs*). *TERs* contain fork pausing elements that influence fork progression and merging. The Rrm3 DNA helicase assists fork progression across *TERs*, counteracting the accumulation of X-shaped structures. The Top2 DNA topoisomerase associates at *TERs* in S phase, and G2/M facilitates fork fusion and prevents DNA breaks and genome rearrangements at *TERs*. We propose that in eukaryotes, replication fork barriers, Rrm3, and Top2 coordinate replication fork progression and fusion at *TERs*, thus counteracting abnormal genomic transitions.

INTRODUCTION

Chromosome replication initiates at multiple origins that fire throughout S phase. Following origin firing, the replication forks move bidirectionally until they fuse with forks coming from adjacent origins (Edenberg and Huberman, 1975). In *E. coli*, chromosome termination takes place within a broad region containing several Tus-*TER* complexes, specialized polar fork barriers confining fork fusion to a site of 270 kb (Duggin et al., 2008). In eukaryotes, replication termination appears to occur randomly within a 4 kb zone (Greenfeder and Newlon, 1992a; Zhu et al., 1992). Two of the three termination regions identified in yeast contain fork pausing elements (Greenfeder and Newlon, 1992a). Certain loci, such as the *RTS1* region and the rDNA locus, exhibit specific termination sites (Brewer and Fangman, 1988; Dalgaard and Klar, 2000). Within these regions, specialized replication fork barriers (RFBs) mediate termination in an orientation-dependent manner, arresting one of the two forks. Fork pausing can destabilize the fork, and RFBs can be associated with chromosome breakage and genomic rearrangements (Kobayashi, 2006; Lambert et al., 2005). Replication forks frequently stall at centromeres (*CENs*) (Greenfeder and Newlon, 1992b), replication slow zones (*RSZs*) (Cha and Kleckner, 2002), tRNA genes or Ty elements (Admire et al., 2006; Lemoine et al., 2005), and regions where collision of transcription and replication occurs (Azvolinsky et al., 2009; Deshpande and Newlon, 1996; Tuduri et al., 2009). The helicase Rrm3, a component of the replisome, facilitates fork progression through nonhistone protein-DNA complexes (Ivessa et al., 2003).

Catenated intertwines can arise when two replicons fuse together (Fields-Berry and DePamphilis, 1989; Wang, 2002). In vivo and in vitro studies have implicated both type IA (Top3) and type II (Top2) topoisomerases in replication termination (Baxter and Diffley, 2008; Cuvier et al., 2008; DiNardo et al., 1984; Suski and Marians, 2008; Wang, 2002). Top3 has been involved in the resolution of sister chromatid junctions, which have also been related to termination structures (Branzei et al., 2006; Chan et al., 2009). Top2 associates with chromosomal regions during S phase (Bermejo et al., 2007) and localizes at *CENs* in metaphase (Bachant et al., 2002). Cells lacking Top2 experience DNA breakage upon cell division (Holm et al., 1989).

We investigated whether in eukaryotes termination occurs at specific chromosomal loci. To identify the chromosomal termination regions, we used genomic approaches to monitor replication fork progression and fusion. We identified 71 termination regions (*TERs*) with an average length of 5 kb. *TERs* contain fork pausing elements. Rrm3 assists fork progression across *TERs*, and in *rrm3Δ* cells, X-shaped intermediates accumulate at *TERs*. Top2, but not Top3, facilitates fork fusion and the resolution of the topological constraints at *TERs*. In *top2* mutants, *TERs* accumulate breaks and rearrangements.

Together, our results contribute to elucidating the mechanisms coordinating chromosome replication termination in eukaryotes and those cellular pathways that control the integrity of *TERs*.

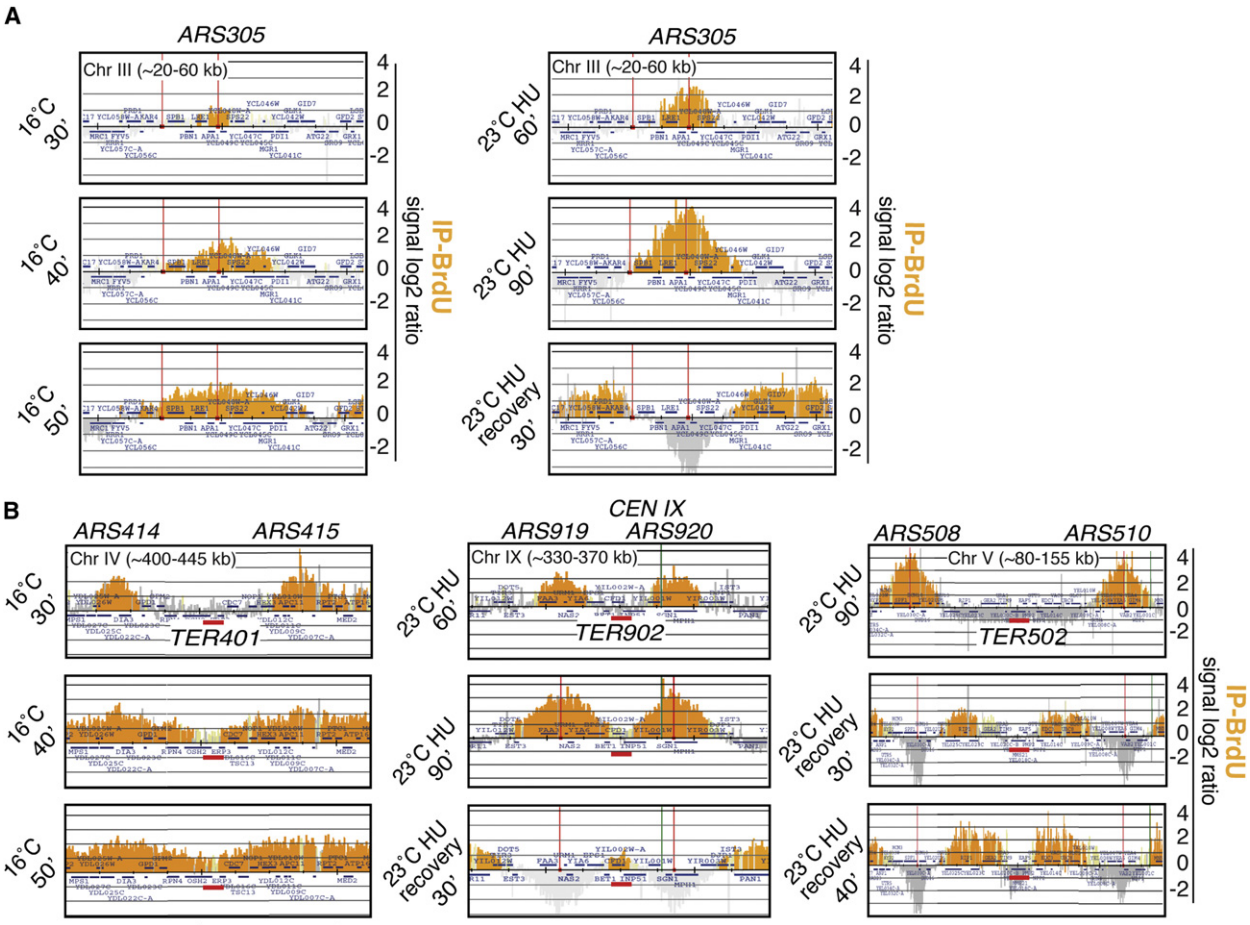

Figure 1. Replication Fork Dynamics and Fusion

(A and B) WT (sy2201) cells were arrested in G1 and released in S phase with BrdU in three different sets of experiments (untreated 16°C, HU, and HU recovery). Orange histogram bars (BrdU) in the y axis represent the average signal ratio of loci significantly enriched in the immunoprecipitated fraction (IP) along the indicated regions in log2 scale (detection p value and change p value are < 0.001; light orange bars should contain at least ten contiguous probes with a p value < 0.001). The x axis shows chromosomal coordinates. *ARS* elements are indicated (red lines), and the blue bars mark the ORFs. Examples of fork movement monitored by BrdU incorporation at *ARS305* with methods 1, 2, and 3 are shown in (A). See Table S2 for the list of the origin-related BrdU peaks. Visualization of three *TERs* using the three methods is shown in (B). Red bars indicate *TERs*. Replication origins and experimental conditions are shown. The green line indicates the centromere. See Figure S1 and Table S3 for *TER* sizes and positions.

RESULTS

Genomic Approaches to Identify *TERs*

We used chromatin immunoprecipitation (ChIP)-chip and bromodeoxyuridine (BrdU) incorporation (Katou et al., 2003) to monitor with time the movement of the BrdU peaks arising from origins of replication and progressively invading adjacent chromosomal regions. With this approach, we were able to identify those chromosomal areas where two fork-related BrdU peaks converged. We defined as termination zones (*TERs*) the minimal unreplicated regions flanked by BrdU peaks arising from adjacent origins of replication. It is expected that the fork fusion sites would lie somewhere within *TERs*. To maximize cell synchronization, we performed our experiments at low temperature or in the presence of hydroxyurea (HU) to slow fork progression. Three sets of experiments were performed (Figure 1A): (1) WT (Table S1) G1 cells were released in BrdU at 16°C, and samples were taken every 10 min for 1 hr; (2) G1 cells were released in BrdU and HU at 23°C, and samples were collected every 30 min for 3 hr; and (3) G1 cells were released in HU for 90 min and then in fresh medium with BrdU at 23°C. Samples were taken every 10 min for 90 min. Under these conditions, we specifically monitored termination of those forks arising from late origins.

Consistent with previous analyses (Raghuraman et al., 2001; Yabuki et al., 2002) (http://www.oridb.org/index.php), we identified 146 BrdU peaks corresponding to early origins and 83 to late origins (Table S2). We also identified 71 *TER*s with an average length of 5 kb (Figure S1 and Table S3). We excluded from our analysis the regions containing BrdU peaks close to telomeres and those termination areas that were either too large or not well defined. Some *TERs* were previously described or inferred from previous analysis (Greenfeder and Newlon, 1992a; Raghuraman et al., 2001; Zhu et al., 1992).

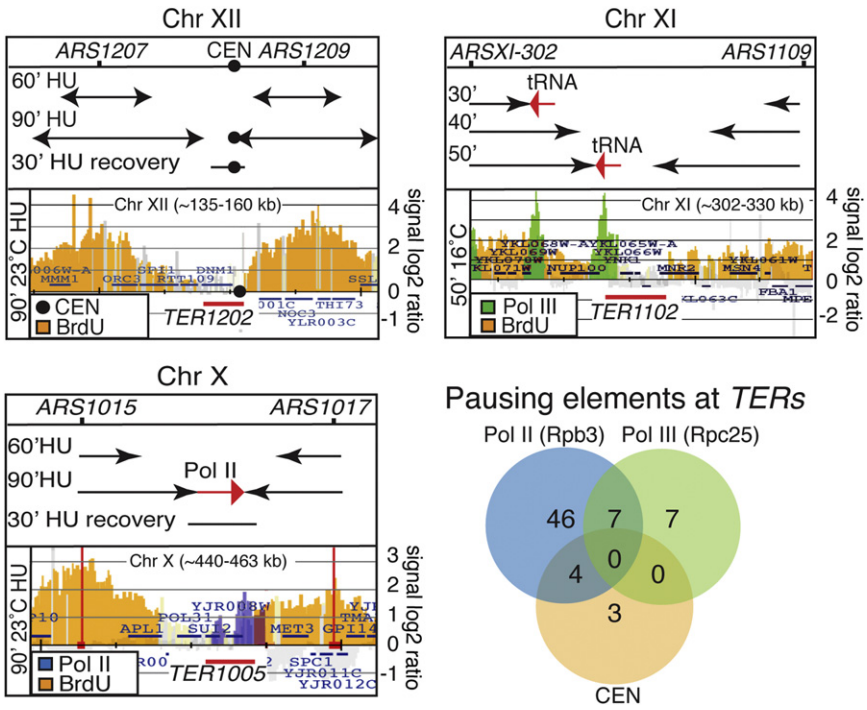

Figure 2. Identification of Pausing Elements at *TERs*

TER1202 (CHRXII), *TER1102* (CHRXI), and *TER1005* (CHRX) are shown as examples. BrdU-labeled forks are indicated in orange and derive from the analysis carried out in strain sy2201 using the conditions for experiment 1 (*TER1102*) or experiments 2 and 3 (*TER1202* and *1005*), respectively. In each panel, the top part shows the extension of fork movements (black arrows) at the indicated time points based on BrdU data. In each panel, the bottom part represents a selected time point when forks reach the *TER* area. The black circle within *TER1202* indicates the centromere. The green peaks in the bottom part of the *TER1102* panel indicate the S phase clusters of the Pol III subunit Rpc25 using strain cy8735. The blue peaks in the bottom part of the *TER1005* panel indicate the S phase clusters of the Pol II subunit Rpb3 using strain cy8519 (see Experimental Procedures for details). Red arrows indicate transcription direction. Red bars mark the *TER* zones. The Venn diagram shows the relative number of *TERs* containing centromere (orange), Pol II (blue), and Pol III (green). See also Table S4 for a list of *TERs* containing pausing elements.

We then investigated whether fork termination at the 71 *TERs* correlated with loci or events that could potentially interfere with fork progression. Since polymerase (Pol) II- and III-mediated transcription interferes with replication (Azvolinsky et al., 2009; Deshpande and Newlon, 1996; Olavarrieta et al., 2002), we performed in S phase ChIP-chip analysis of Rpb3 and Rpc25, which are subunits of RNA Pol II and III, respectively. The S phase enrichment of Rpb3 at mRNA genes or of Rpc25 at tRNA genes and long terminal repeats (LTRs), besides revealing transcription activity, may also mark potential fork pausing regions. We included in our analysis also those pausing elements that have been previously annotated (such as *CENs*, *RSZs*, and noncoding RNA genes) (Cha and Kleckner, 2002; Deshpande and Newlon, 1996; Greenfeder and Newlon, 1992b). Almost all *TERs* contain one or more potential replication pausing elements (examples in Figure 2 and Table S4). In fact, in 64 of 71 cases, the *TER* zones contained transcription clusters, and in 7 of 71 cases, *CENs* were located within *TERs*. We did not detect obvious features in 4 of 71 *TERs*, although in these cases transcription clusters were within a range of 1–3 kb away from the *TER* zones (asterisk in Table S4). Overall, 67 of 71 *TERs* contained one or more pausing elements that might affect fork progression (Table S4). The association between pausing elements and *TERs* is greater than random ($p = 0.00021$) (Table S5).

Yeast replication pause sites have been identified by mapping the high-occupancy sites of DNA polymerase ε (Polε) in WT and *rrm3Δ* cells (Azvolinsky et al., 2009). We found that 47 of 71 *TERs* correlate with high-occupancy Polε sites observed in WT and/or in *rrm3Δ* mutants, further suggesting that the replisome physiologically stalls at *TERs* (Figure S2 and Table S4).

At *TERs*, in most of the cases, transcription was on a head-on orientation with only one of the two converging forks, even at those *TERs* that contained more than one transcription cluster. Even if we cannot always predict which of the two converging replication forks is slowed down, we notice that in 62 of 71 cases, the pausing elements could slow either the left or the right forks, but not both (Figure 2 and Table S4). This includes the four *TERs* in which the pausing elements were adjacent (asterisk in Table S4) and five out of seven *CEN*-containing *TERs* where one of the two forks reaches the *CEN* before the other. Out of the nine remaining *TERs*, in two cases (*TER704* and *TER1604*), the right and left forks seemed to converge at *CENs* simultaneously; in one (*TER1503*), the polarity was dubious; and in six cases (*TER304*, *702*, *801*, *1101*, *1601*, and *1602*), termination was associated with two divergent Pol III-transcribed units that potentially paused both converging forks.

Rrm3 Is Required for Fork Progression across *TERs*

We used 2D gels to visualize replication intermediates at *TERs* in WT and *rrm3* cells (Figures 3 and S3, Table S4, and data not shown). The visualization of replication termination intermediates is hampered by their fast turnover and by fork velocity. We found that the best approach to visualize termination structures is the 2D gel technique coupled with psoralen-crosslinking treatment. These procedures maximize the visualization of the intermediates resulting from the converging of the two forks while selectively resolving fork-related cruciform intermediates (Lopes et al., 2003; M. Lopes and M.F., unpublished data), which are unrelated to replication termination and might interfere with the visualization of termination structures. We focused on two classes of *TERs*, those with (21 of 71) Rrm3-dependent pause sites, such as *CENs* and tRNA genes, and those without (46 of 71), which correlate with the presence of Pol II clusters (Azvolinsky et al., 2009).

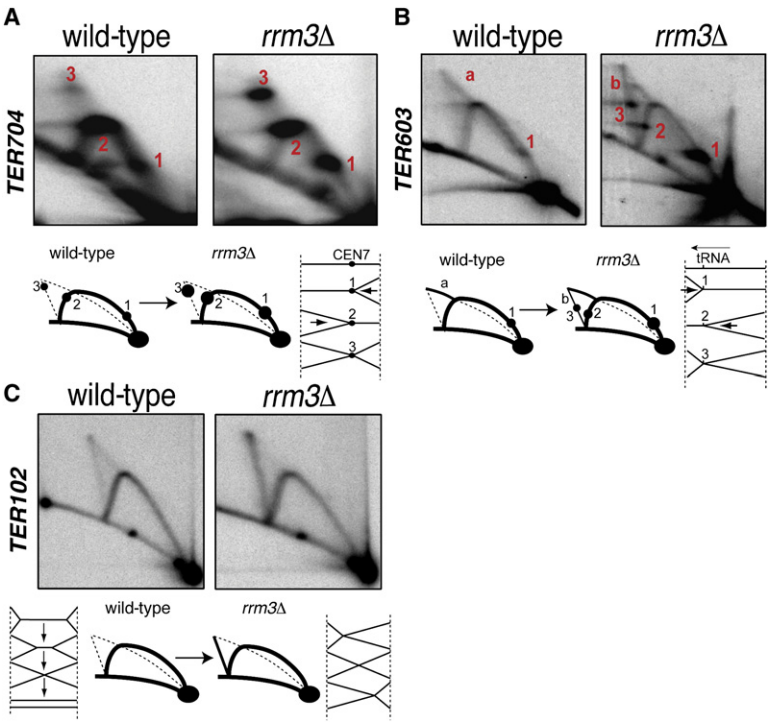

Figure 3. Rrm3 Contributes to Fork Progression across *TERs*

(A–C) WT (sy2209) and *rrm3Δ* (cy6807) cells were presynchronized in G2 with nocodazole and released in α factor. Cells were then released in S phase at 23°C, and samples were collected at 40 min. Genomic DNA was analyzed by 2D gels. Schematic representations of the different fork pausing and termination signals are shown. The red letters in (B) indicate double Y and Xs, respectively. The red numbers indicate pausing sites (see text for details). Relative BrdU maps, restriction digestion strategy, and 2D gel quantification are shown in Figure S3.

In WT cells, at *TER704*, two spots (1 and 2 in Figure 3A) appeared on the Y-arc, reflecting fork pausing at *CEN7*. We also observed a diffuse termination cone signal with a defined X-spot (3), likely reflecting delayed termination at *CEN7*. *rrm3Δ* cells exhibited an increase in the intensity of Y- and X-spots, consistent with their role in facilitating replication across pause sites (Ivessa et al., 2003). We obtained analogous results in other *CEN*-associated *TERs* (*TER402*, *1504*, and *1604*) (data not shown).

TER603 contains a tRNA gene, and WT cells accumulated a pausing signal on the Y-arc (1 in Figure 3B) (Deshpande and Newlon, 1996) and termination intermediates (a). In *rrm3Δ* cells, the intensity of the Y-spot increased and another pause signal appeared (2) because Rrm3 facilitates fork progression even at tRNA genes transcribed codirectionally with the fork (Ivessa et al., 2003). *rrm3Δ* cells also exhibited a transition of the termination intermediates from a double-Y conformation (a) to an X conformation (b) (Figure 3B). Moreover, an asymmetric X-spot accumulated (3) due to termination at the tRNA site. We obtained analogous results with *TER1102* and *1503* (data not shown).

The accumulation of X-shaped converging forks in *rrm3Δ* cells may result from slowing down of one of the two forks at a pause site, which is then more likely to become a termination site as the other converging fork approaches. However, this does not rule out that Rrm3 might also directly assist fork fusion later at termination.

The majority of *TERs*, including *TER102*, contain a Pol II-transcribed gene that slows down forks independently of Rrm3 (Azvolinsky et al., 2009). Fork pausing throughout highly transcribed RNA Pol II genes is not confined to specific sites and occurs over the entire ORF region (Azvolinsky et al., 2009; Bermejo et al., 2009); thus, it does not always generate obvious discrete spots on the Y-arc of the 2D gel. While WT cells accumulated at *TER102* a cone signal due to random termination (Figure 3C) (Greenfeder and Newlon, 1992a), *rrm3Δ* mutants accumulated Xs. A possible interpretation, although not exclusive, is that these X-shaped molecules result from the impaired fusion of converging forks. Indeed, partially replicated double-Y termination intermediates are progressively converted into fully replicated Xs and then into replicated linear molecules (Figure 3C). While in WT cells, the conversion of Xs into linear intermediates is likely very fast, as X molecules do not accumulate, *rrm3Δ* cells might be delayed in this termination step since these unresolved termination structures accumulate and persist during S phase. Similar results were seen for *TER101*, *202*, *301*, *502*, *601*, *902*, *1002*, *1005*, *1303*, and *1608* (data not shown).

X-shaped structures can also arise as a result of recombination (Liberi et al., 2005; Schwacha and Kleckner, 1994). We failed to observe a significant difference between the level of Xs at *TERs* in *rrm3Δ* and *rrm3Δ rad51Δ* mutants, thus suggesting that these X-structures did not arise from recombination (data not shown). Moreover, the X-shaped structures were detected at *TERs* but not at *TER*-flanking regions (data not shown), further suggesting that they are related to termination events.

In conclusion, we analyzed by 2D gel 20 *TERs* corresponding to the three classes of *TER*. In all of them, termination intermediates were visualized, thus validating our genomic approaches. Moreover, in all 20 cases, termination signals were enhanced in the absence of Rrm3, even at those *TERs* that do not contain obvious Rrm3-dependent pausing elements.

Top2 Is Recruited at *TERs* and Facilitates Replication Termination

Top1, Top2, and Top3 move with forks (Bermejo et al., 2007) (data not shown). Topoisomerases might approach *TERs* by traveling with the forks or associate with *TERs* before or after the arrival of converging forks. The presence of topoisomerases at *TERs* may not be confined to S phase, as topological constraints could persist after S phase (Fields-Berry and DePamphilis, 1989; Holm et al., 1985). We investigated by ChIP-chip the presence of Top2 and Top3 at *TERs*, both in S and in G2/M cells.

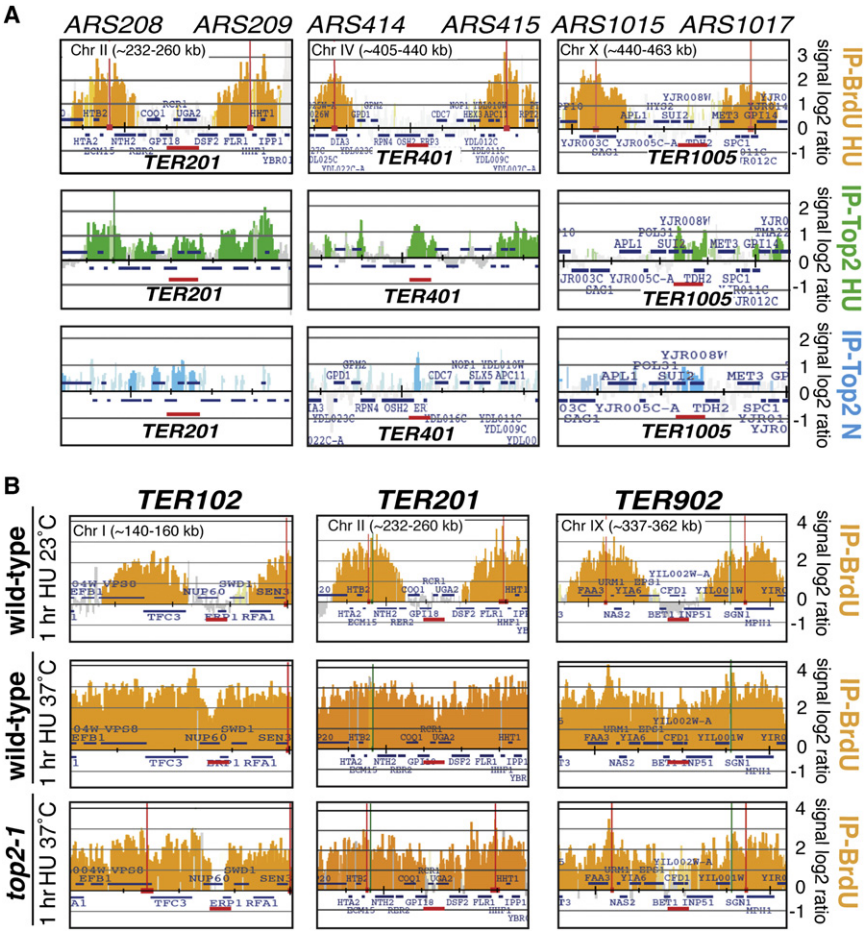

Figure 4. Top2 Is Required for Efficient Replication Termination

(A) The ChIP-chip data are described as in Figure 1. Top2-10Flag (cy7315) cells were arrested in G1 with α factor and released at 23°C in the presence of HU for 1 hr or in the presence of nocodazole for 3 hr. Samples were collected at the indicated time points and processed for ChIP-chip analysis. As a control, we show the BrdU maps (in orange) that correspond to forks that have experienced 1 hr in HU. Green histogram bars represent the Top2 clusters in HU (IP-Top2 HU), and the blue ones indicate the Top2 clusters in nocodazole (IP-Top2 N). Red bars indicate the *TER* zones.

(B) WT (sy2201) and *top2-1* (cy7421) cells were released from α factor in YPD with BrdU and HU at 37°C for 1 hr. BrdU maps of WT cells experiencing HU treatment at 23°C are also shown. Red bars indicate the *TER* zones. List of *TERs* containing Top2 clusters is shown in Table S4 and the relative statistical analysis in Table S5.

Cells were released from G1 in HU or nocodazole. No enrichment was observed for Top3 at *TERs* under both conditions (data not shown). Top2 clusters were observed in S phase and G2/M but not in G1 (Bermejo et al., 2007). The majority of S phase Top2 clusters are related to fork-associated Top2 and S phase-transcribed genes (Bermejo et al., 2009). We found that Top2 associates with 51 of 71 *TERs* in HU ($p = 0.00047$) and in 55 of 71 in nocodazole ($p = 0.0065$) even at those *TERs* that do not contain transcription units (Figure 4A and Tables S4 and S5). We obtained similar results when S phase cells were grown with a different carbon source (53 of 71, $p = 0.0000056$) (Tables S4 and S5). We failed to visualize Top2 in 4 of 71 *TERs*. Hence, Top2 associates with the majority of *TERs* before fork arrival and persists in G2/M.

We then investigated whether fork fusion at *TERs* was affected in *top2* mutants. We analyzed the convergence of the BrdU-labeled forks in WT and *top2* cells released from G1 into HU at the restrictive temperature for 1 hr. Only *TERs* within an interorigin spacing of ≤20 kb could be considered for this analysis. While WT cells efficiently completed replication at *TER102*, *103*, *201*, *403*, *404*, *902*, *1005*, *1202*, *1302*, *1401*, and *1604* (Figure 4B and data not shown), in *top2* mutants, the same *TERs* exhibited unreplicated regions with an approximate size of 1 kb. Since in *top2* mutants the timing of origin firing is not delayed compared to WT cells (Bermejo et al., 2007), this result suggests that the replication of the last 1 kb at *TERs* is somewhat limiting in *top2* cells, perhaps due to the topological constraints generated at the point where forks converge. In support of this conclusion, kinetics analysis showed that within the same replicon, specifically the fork experiencing termination was delayed, but not the other one (data not shown). This observation further confirms previous findings indicating that sister replication forks can be uncoupled (Doksani et al., 2009; Wang et al., 2008). Replication termination at *TERs* was delayed but not prevented in *top2* mutants, as the forks converged later on (data not shown).

In *top2* mutants, at the restrictive temperature, the chromosomes remain entangled and undergo breakage during cell division, as shown by pulse field gel electrophoresis (PFGE) (Figure 5A). Conversely, we failed to detect obvious differences between WT and *top3* mutants. We then investigated in *top2* cells by PFGE a 109 kb EagI fragment of CHR III that includes two *TERs* between *ARS305* and *ARS307*. In WT cells, the genomic fragment was fully replicated by 1 hr, while in *top2* mutants it remained in the wells even at 4 hr and later accumulated DNA breaks (Figure 5B). The appearance of DNA breaks correlated with the decrease of the signal in the wells. We note that in *top2* mutants at 37°C, the nocodazole block persists for no more than 3 hr (Figure S4A). Again, we failed to visualize entangled chromosomes and double-strand break (DSB) formation in *top3* mutants. To address whether at least a fraction of DNA breaks in *top2* mutants may be related to abnormal termination, we deleted *ARS305* and *ARS306* to prevent fork fusion in the EagI fragment. DSB formation in *top2-1 ars305Δ ars306Δ*, compared to *top2-1* mutants, was reduced about

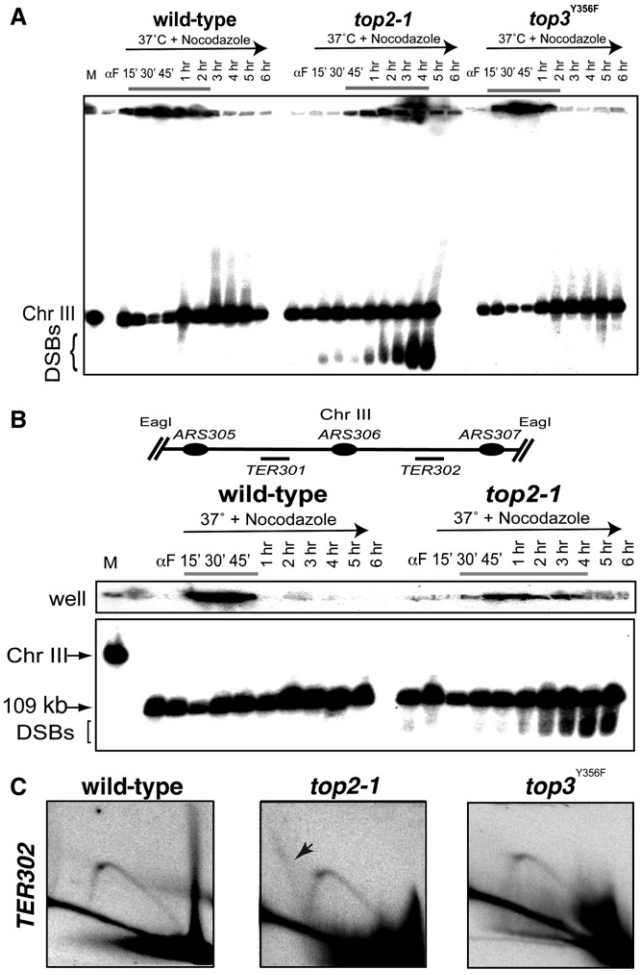

Figure 5. Top2 Is Required for Chromosome Resolution

(A) WT (cy7627), *top2-1* (cy7671), and *top3*^{Y356F} (cy7629) cells were arrested in G1 with α factor and released in S phase in YP + Gal at 37°C in the presence of nocodazole. Genomic DNA was extracted in agarose plugs at the indicated time points. Yeast chromosomes were separated by PFGE and analyzed by Southern blotting with the *TER302* probe. M indicates the chromosome marker. DSBs indicate double-strand breaks.

(B) Agarose plugs were digested with EagI. Schematic representation of the analyzed region is shown.

(C) WT (cy7627), *top2-1* (cy7671), and *top3*^{Y356F} (cy7629) were released in S phase at 37°C, and different samples (30, 40, and 50 min) were pulled together to increase the chance to visualize the replication intermediates. DNA (30 μg) was digested with HindIII and PstI and analyzed by 2D gels using *TER302* probes. FACS, PFGE, and 2D gels are also shown in Figure S4.

3-fold at the EagI fragment but not at other regions (Figure S4B and data not shown). The residual breaks are likely due to faulty coordination between replication and transcription (Bermejo et al., 2009) and/or to rare termination events perhaps resulting from firing of the dormant *ARS302-303-320* origins cluster (Wang et al., 2001), although we failed to detect by 2D gel any obvious bubble structure under our conditions.

We then analyzed the replication intermediates at *TER302* in WT, *top3*, and *top2* cells at the restrictive temperature (Figure 5C). WT cells exhibited Ys but no obvious termination structures, perhaps because of their fast turnover at 37°C. We note that termination structures can be seen in the same region in WT cells at 23°C (data not shown). *top3* mutants exhibited 2D gel profiles similar to WT. Conversely, *top2-1* mutants accumulated additional fully duplicated X-intermediates only at *TERs* (Figure 5C) but not at other genomic locations (Figure S4C). These structures likely represent X-shaped entangled precatenane derivatives resulting from aberrant termination (Bermejo et al., 2007). We obtained analogous results for *TER704* and *TER1504* (data not shown). We conclude that Top2, and not Top3, plays a major role in the resolution of S phase chromosomes and that genetic defects affecting the resolution process correlate with formation of DNA breaks.

Top2 Protects the Integrity of *TERs*

Top2 prevents the expression of fragile sites, and in *top2* mutants, aberrant S phase events cause DNA break formation during cell division (Baxter and Diffley, 2008; Bermejo et al., 2007, 2009; Holm et al., 1985). Hence, we investigated whether Top2 prevents abnormal transitions at *TERs*. Histone H2A phosphorylation on Ser129 (γH2A) marks nicks/gaps and DNA breaks (Lydall and Whitehall, 2005; Vidanes et al., 2005). We analyzed by ChIP-chip the γH2A clusters in *top2-1* cells at the restrictive temperature following cell division. γH2A clusters significantly accumulate throughout the genome at Top2-bound regions (Bermejo et al., 2009). Accordingly, we found γH2A peaks also at 37 of 67 Top2-bound *TER* regions (Figure 6A and Table S4).

Hence, *TERs*, like other genomic loci (Bermejo et al., 2009), express DNA fragility during cell division. To visualize potential chromosomal instability at *TERs* owing to *top2* mutations before chromosome segregation, we performed comparative genome-wide analysis in *top2* mutants experiencing one round of DNA synthesis. Comparative genome hybridization (CGH) was performed in WT and *top2* cells released from G1 in S phase at 25°C (reference-DNA sample) or 37°C (test-DNA sample) with nocodazole. This approach allows us to measure those genomic locations where test DNA is present in an equal, reduced, or increased amount compared to the reference DNA.

Thirteen loci exhibited deletions and/or amplifications in *top2* mutants (Figures 6B and 6C and Table S6). These include four *TERs* (*TER304*, *404*, *502*, and *801*), three hypothetical *TERs* (our analysis did not allow us to define a clear *TER* in these regions), three Ty elements, the left subtelomeric region and the right telomere of CHR I, and partially the rDNA locus. (The majority of the rDNA locus, as well as other repetitive sequences, is not present in the array). We note that *TER304* is a known genome instability site (Lemoine et al., 2005) and that rDNA instability was already described in *top2* mutants (Christman et al., 1988; Holm et al., 1989). Hence, within a cell population lacking a functional Top2 activity, there are specific chromosome regions that are more subject than others to chromosome instability, and one-third of these loci are *TERs.* Moreover, these data indicate that in *top2* mutants, a fraction of *TERs* already exhibited abnormalities at the end of S phase, while the majority of *TERs* accumulated γH2A later on, during cell division.

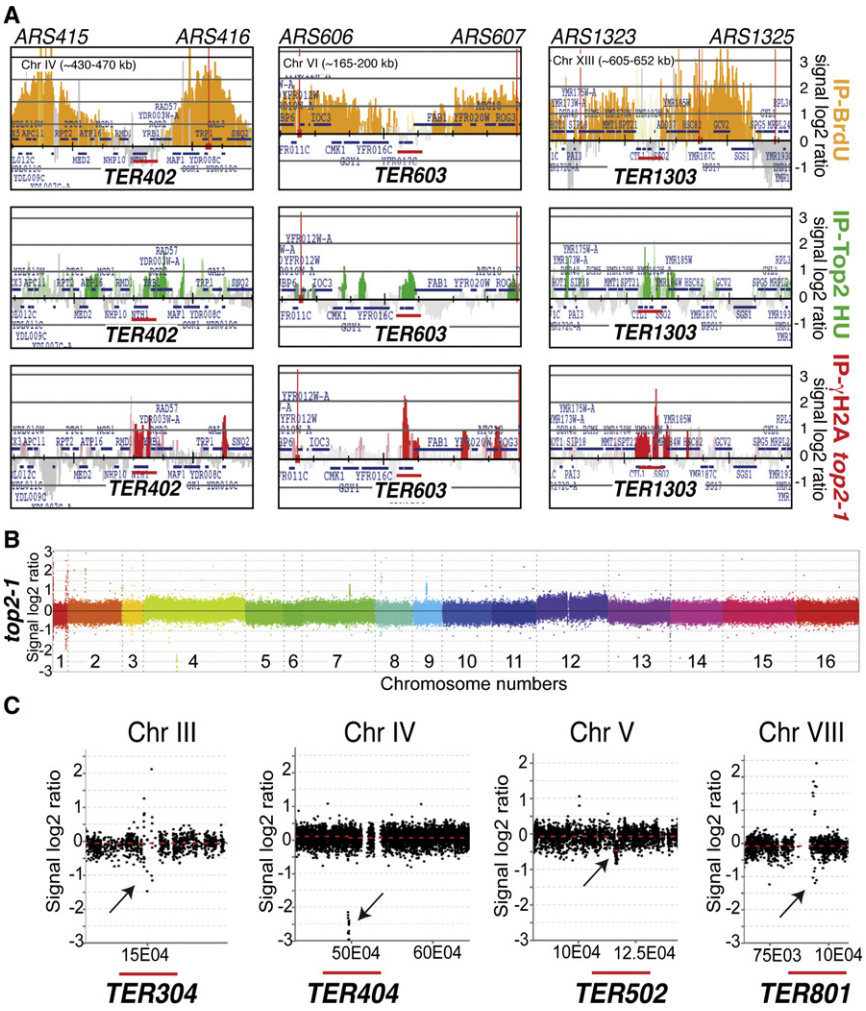

Figure 6. Top2 Prevents Fragility at *TERs*

(A) *top2-1* (cy8423) cells were released from G1 in S phase at 37°C. The sample was collected after 150 min (following cell division) and processed for ChIP-chip with antibodies against γH2A. The red histogram bars represent the γH2A clusters. BrdU-labeled forks (orange, IP-BrdU) and Top2 peaks (green, IP-Top2 HU) obtained from independent experiments are also shown. The red bars mark the *TERs*. See also Table S4.

(B) *top2-1* (cy7671) cells were released from G1 in S phase at 25°C or 37°C in the presence of nocodazole to compare the relative genomes within one cell cycle. Samples were collected after 2.5 hr and processed for CGH analysis. The plot of the log2 ratio value on y axis shows DNA copy number changes between test-DNA and reference-DNA. The different colors represent all 16 chromosomes, and the corresponding number is indicated.

(C) SignalMap ver1.9 (NimbleGen) magnification of four regions detected by CGH. Plot of the log2 ratio value on y axis shows DNA copy number changes. The x axis shows chromosomal coordinates. Black arrows indicate sites of genomic instability. Red bars indicate position of *TER* sites. Genome instability regions are also shown in Figure S1 and Table S6.

DISCUSSION

We showed that eukaryotic replication termination occurs at *TERs* containing fork barriers. There are intriguing analogies with prokaryotes where specific termination sites and polar pausing elements influence termination. It is possible that fork barriers have passively localized through evolution in proximity of *TERs*, because if replication forks have to pause, it is least disadvantageous when this occurs at a site where forks are converging. Alternatively, evolution has brought fork barriers at *TERs* to influence fork fusion. Intriguingly, we note that deleting an efficient origin causes the relocalization of fork fusion from the original *TER* to another pausing element (data not shown), thus suggesting that the site of termination is influenced by the presence of pause sites.

Our findings also suggest that the polarity of fork barriers had an evolutionary impact on chromosome replication and on *TER* integrity. Indeed, using the yeast comparative genomics database, we notice that in 5 out of 6 *TERs* (*TER304*, *702*, *801*, *1601*, and *1602*) containing two divergent Pol III-dependent pause sites (tRNA/LTR), one of them is totally or partially not conserved (Figure S5) (Ted Weinert, personal communication). On the other hand, those 58 *TERs* that contain polar barriers have conserved the pause sites in other yeasts. We excluded from the analysis the seven *TER*-containing *CENs*, as *CENs* are known to rapidly diverge in evolution (Henikoff et al., 2001) (and on the other side represent bipolar pausing elements). This correlation ($p = 0.00000465$) further suggests the existence of an evolutionary pressure against *TER*-containing pause sites on both strands, perhaps to avoid genome instability events. In this view, we note that *TER502* (the remaining unconserved *TER*), *304*, and *801* are unstable in *top2* mutants, as shown by CGH analysis (Figure 6C), *TER304* and *TER702* are hot spots for genome rearrangements (Admire et al., 2006; Lemoine et al., 2005), and γH2A accumulates in *TER304*, *502*, *702*, and *1601* (Table S4). It will be of interest to address how replication termination is achieved when transcription is dispensable, as in the frog embryonic cell cycle. We also note that *TERs* seem to correlate with low-nucleosome regions ($p = 0.07$) (Table S5).

Based on in vivo and in vitro studies, both Top2 and Top3 have been suggested to play a role in replication termination (Baxter and Diffley, 2008; Branzei et al., 2006; Chan et al., 2009; Cuvier et al., 2008; DiNardo et al., 1984; Suski and Marians, 2008; Wang, 2002). Our data argue against a major contribution for Top3 at replication termination at the chromosomal level; rather, they pinpoint the importance of Top2 in mediating topological transitions at *TERs*. Although alternative possibilities could be envisaged, we propose the following three-step model (Figure 7).

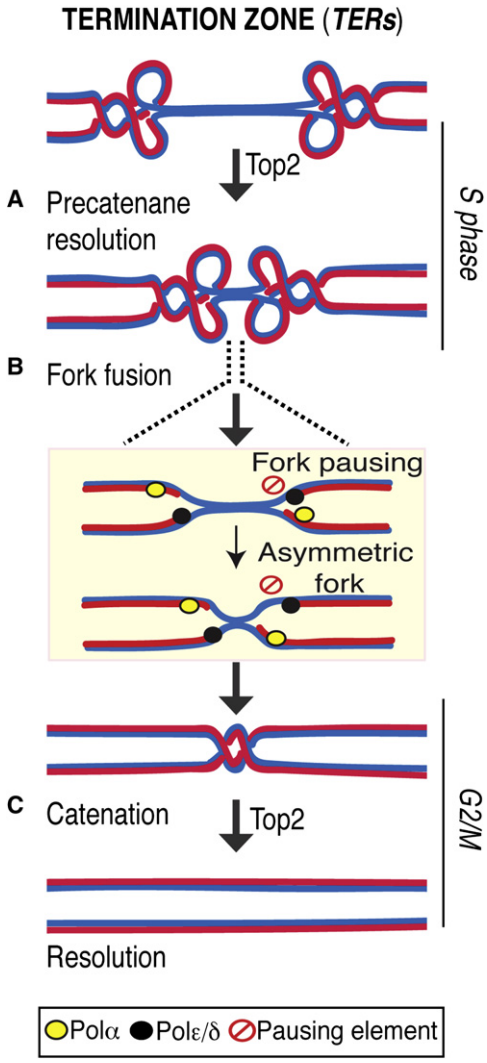

Figure 7. A Model for Replication Termination

(A) Precatenane resolution: Top2 mediates fork progression at the *TER* zone by resolving precatenanes behind the forks.

(B) Fork fusion: the right fork stalls at a pausing site (pausing element, red symbol) and emerges with an asymmetric conformation. The leading polymerase (black oval) and the lagging apparatus (yellow oval) are shown.

(C) Catenation: Top2 then resolves the last catenation at *TERs* before DNA segregation, allowing chromosome resolution.

Step A: Rrm3, Top1, and a fraction of Top2 travel with the fork (Azvolinsky et al., 2006; Bermejo et al., 2007). Rrm3 facilitates fork progression across pausing sites (Ivessa et al., 2003), while Top1 and Top2 are both needed to resolve the torsional stress ahead of the fork generated during fork progression: while Top1 resolves positive supercoiling ahead of the fork (Wang, 2002), also contributing to prevent interference between replication and transcription (Tuduri et al., 2009), Top2 likely acts behind the fork to resolve precatenanes (Lucas et al., 2001; Wang, 2002). When forks approach the termination zone, the topological constraints at converging forks can no longer be resolved by Top1 (Fields-Berry and DePamphilis, 1989), and therefore the only option for fork progression is to rely on Top2 activity. This is consistent with the observation that *top2* mutants are selectively delayed in completing the last portion of replication but not the bulk of DNA synthesis. However, we cannot rule out that the topological architecture of the termination zone (e.g., chromosome loops) specifically needs Top2 activity for resolution. Indeed, a subpopulation of Top2 is also bound to *TERs* in early S phase, perhaps due to the affinity of Top2 for nucleosome-free regions ($p = 2.10E - 58$). Moreover, other S phase Top2 clusters have recently been suggested to correlate with the formation of chromosome loops (Bermejo et al., 2009). We found that the Top2 clusters at *TERs* are established already at the *cdc7*-dependent step and are not influenced by origin firing (data not shown), thus suggesting that *TERs* represent *cis* chromosomal elements that undergo topological transitions requiring Top2 activity.

Step B: When fork fusion occurs, the lagging polymerase encounters the leading strand polymerase from the opposite fork, thus physically occupying the remaining unreplicated region (Sundin and Varshavsky, 1981). It is still unclear how the replisome is dismantled and how fork fusion occurs. Perhaps the presence of polar fork barriers may guarantee that the two forks do not converge simultaneously, thus ensuring that at least one of the two forks emerges from the pausing region with asymmetric leading and lagging strands before fusing with the other fork. This is consistent with the finding that stalled forks exhibit an asymmetric configuration (Gruber et al., 2000; Sogo et al., 2002). Rrm3 could simply facilitate fork progression at the pause sites located within the *TERs*. However, we cannot exclude the possibility that Rrm3 actively participates at fork fusion, as suggested by the finding that unresolved termination structures accumulate even at those *TERs* that do not contain obvious Rrm3-dependent pause elements.

Considering that (1) the termination context might be ideal for fork reversal as topological constraints accumulate and the replisome must be dismantled (Postow et al., 2001), (2) the Mec1-Rad53 checkpoint pathway prevents fork reversal when forks stall (Sogo et al., 2002), and (3) checkpoint factors have been implicated in mediating termination at the rDNA locus (Mohanty et al., 2006), it is tantalizing to speculate that the Mec1 checkpoint pathway somewhat prevents aberrant fork transitions, such as fork reversal, at termination zones.

Step C: Fork fusion then gives rise to catenated sister chromatid junctions that have to be resolved before segregation. We propose that this last step is mediated by a subpopulation of preassembled *TER*-associated Top2 that can persist even after S phase. It is also possible that Top2, at least in a fraction of *TERs*, is loaded at the beginning of mitosis. Given that the catenated junction might be mobile and spread along the chromosomes (Spell and Holm, 1994), the presence of preassembled Top2 might be needed to confine and coordinate its resolution at the *TER* loci, perhaps through SUMO-mediated regulation (Bachant et al., 2002; Dawlaty et al., 2008).

According to the model proposed, the transient accumulation of topological constraints might facilitate abnormal transitions (Hiasa and Marians, 1994) that could lead to amplification or deletion of *TER* sites. Moreover, the proper resolution of catenated sister chromatids would be impaired in *top2* cells and,

following cell division, DNA breaks, and aberrant segregation will be expected (Baxter and Diffley, 2008; Bermejo et al., 2007; DiNardo et al., 1984; Holm et al., 1989).

Together, our data provide a framework for understanding the eukaryotic molecular mechanisms that control replication termination and coordinate replication with transcription and topological dynamics.

EXPERIMENTAL PROCEDURES

Yeast Strains and Growing Conditions

All strains (Table S1) are isogenic derivatives of *W303-1A*. All epitope tags (10Flag and 6PK) were fused to the C terminus of the protein of interest. Strains were grown in YPD and cells were arrested in G1 by α factor (2 μg/ml) or in G2/M by nocodazole (10 μg/ml). HU was added at 0.2 M. Overexpression of the dominant-negative version of Top3 was induced for 3 hr by Galactose 2% in YP + Raffinose 2% media. BrdU was added as previously described (Katou et al., 2003). Rpc25 and Rpb3 subunits were analyzed by ChIP-chip following 1 hr in HU.

Pulse Field Gel Electrophoresis

DNA plugs were prepared as described (Lengronne et al., 2001). Yeast chromosomes were separated by PFGE (Gene Navigator System, Amersham, Munich), and electrophoresis was performed for 15 hr at 200 V with 90 s pulses, followed by 9 hr with 125 s pulses, in TBE 0.5X at 14°C. Plug digestion was performed according to New England BioLabs (Ipswich, MA) and previously described (Azvolinsky et al., 2006).

Psoralen-Crosslinking, DNA Extraction, and 2D Gel Technique

Genomic DNA extraction was performed according to the QIAGEN Genomic DNA Handbook. DNA psoralen-crosslinking and 2D gel procedure were described (Doksani et al., 2009). Quantifications were done using ImageQuant 5.2 (Molecular Dynamics).

Probes are obtained by PCR using the following oligos: *TER102*: Fw TCTGCGCCAAGCAAAGATTC, Rv TTTCCTTGCGTCTGATTCGG. *TER603*: Fw GAATGCCCGAGCCCTAAAAA, Rv ATGTGAGCCATCTGGAAAGG. *TER704*: Fw TGTGCACATCTTGCCCATTA, Rv GCCTCTATCACTGCAAAGTG. *TER302*: Fw GAAGGTTCAACATCAATTGATTGATTCTGCCGCCATGATC, Rv GCTTCC CTAGAACCTTCTTATGTTTTACATGCGCTGGGTA.

ChIP-Chip Analysis

S. cerevisiae oligonucleotide microarrays were provided by Affymetrix (Santa Clara, CA) (*S. cerevisiae* Tiling 1.0R, P/N 900645). BrdU and protein ChIP-chip analyses were carried out as described (Bermejo et al., 2009). Pol2 (Polε) ChIP-chip analysis was performed as described (Azvolinsky et al., 2009).

Comparative Genome Hybridization

Roche-Nimblegen (Madison, WI) 385K Yeast Whole-Genome Tiling arrays were used to perform CGH analysis. Experimental processing was performed according to Roche-Nimblegen protocol, data elaboration using the NimbleScan v2.4 software (Roche-Nimblegen), and the analysis using the embedded packages DNAcopy and segMNT.

Statistical Methods

Evaluation of the significance of the presence of protein-binding peaks and pausing elements within *TERs* (Table S5) was performed by confrontation against a null hypothesis model generated with a Montecarlo-like simulation.

For each data set (binding clusters of a specific protein or set of pausing elements), we produced 1000 randomizations of the positions of the features, maintaining unchanged the number and size of the genomic areas covered within each chromosome; the number of peaks and features with random positions within the *TERs* was then counted and taken as score for each iteration. The distribution of these random scores was validated to be approximately normal (|Skew| < 0.25 and |Kurtosis excess| < 0.25), and then the average and standard deviation for this distribution were taken as null hypothesis.

The increase or decrease ratios for the scores of the actual positions with respect to the expected value for the null hypothesis (defined as the average score of random attempts) was then calculated, and the p values for the drift were estimated as Standard Normal CDF of $\frac{|actual - mean|}{deviation}$.

Evaluation of significance of overlaps in sets (i.e., for the number of nonconserved *TERs* versus the *TERs* containing divergent pausing elements) was performed by means of the Fisher's exact test.

Genomic profiles of all the proteins studied can be accessed from http://bio.ifom-ieo-campus.it/supplementary/Fachinetti_et_al_MOLCELL_2010.

ACCESSION NUMBERS

Experimental data are available on Gene Expression Omnibus database with accession number GSE19061.

SUPPLEMENTAL INFORMATION

Supplemental Information includes five figures and six tables and can be found with this article online at doi:10.1016/j.molcel.2010.07.024.

ACKNOWLEDGMENTS

We thank A. Verreault and E. Schwob for reagents; Ted Weinert for communicating unpublished results; D. Branzei, M. Lopes, and Y. Doksani for suggestions and critical reading of the manuscript; and all members of our laboratories for discussions. We thank M. Cesaroni for *TER* sequence analysis, M. Saponaro for technical advice, and F. Ciccarelli for suggestion on evolution analysis. Work in the M.F. laboratory is supported by grants from Italian Association for Cancer Research, Italian Foundation for Cancer Research, Telethon-Italy, European Community, and Italian Ministry of Health. D.F. was supported by an AIRC fellowship. Work in K.S.'s laboratory is supported by a grant of the Genome Network Project and Grant-in-Aid for Scientific Research (S) from the MEXT, Japan. Y. Katou is a GCOE research associate. Work in V.A.Z.'s laboratory is supported by NIH grant R37 029638.

Received: February 23, 2010
Revised: May 5, 2010
Accepted: June 8, 2010
Published: August 26, 2010

REFERENCES

Admire, A., Shanks, L., Danzl, N., Wang, M., Weier, U., Stevens, W., Hunt, E., and Weinert, T. (2006). Cycles of chromosome instability are associated with a fragile site and are increased by defects in DNA replication and checkpoint controls in yeast. Genes Dev. *20*, 159–173.

Azvolinsky, A., Dunaway, S., Torres, J.Z., Bessler, J.B., and Zakian, V.A. (2006). The S. cerevisiae Rrm3p DNA helicase moves with the replication fork and affects replication of all yeast chromosomes. Genes Dev. *20*, 3104–3116.

Azvolinsky, A., Giresi, P.G., Lieb, J.D., and Zakian, V.A. (2009). Highly transcribed RNA polymerase II genes are impediments to replication fork progression in Saccharomyces cerevisiae. Mol. Cell *34*, 722–734.

Bachant, J., Alcasabas, A., Blat, Y., Kleckner, N., and Elledge, S.J. (2002). The SUMO-1 isopeptidase Smt4 is linked to centromeric cohesion through SUMO-1 modification of DNA topoisomerase II. Mol. Cell *9*, 1169–1182.

Baxter, J., and Diffley, J.F. (2008). Topoisomerase II inactivation prevents the completion of DNA replication in budding yeast. Mol. Cell *30*, 790–802.

Bermejo, R., Doksani, Y., Capra, T., Katou, Y.M., Tanaka, H., Shirahige, K., and Foiani, M. (2007). Top1- and Top2-mediated topological transitions at replication forks ensure fork progression and stability and prevent DNA damage checkpoint activation. Genes Dev. *21*, 1921–1936.

Bermejo, R., Capra, T., Gonzalez-Huici, V., Fachinetti, D., Cocito, A., Natoli, G., Katou, Y., Mori, H., Kurokawa, K., Shirahige, K., and Foiani, M. (2009).

Genome-organizing factors Top2 and Hmo1 prevent chromosome fragility at sites of S phase transcription. Cell *138*, 870–884.

Branzei, D., Sollier, J., Liberi, G., Zhao, X., Maeda, D., Seki, M., Enomoto, T., Ohta, K., and Foiani, M. (2006). Ubc9- and mms21-mediated sumoylation counteracts recombinogenic events at damaged replication forks. Cell *127*, 509–522.

Brewer, B.J., and Fangman, W.L. (1988). A replication fork barrier at the 3′ end of yeast ribosomal RNA genes. Cell *55*, 637–643.

Cha, R.S., and Kleckner, N. (2002). ATR homolog Mec1 promotes fork progression, thus averting breaks in replication slow zones. Science *297*, 602–606.

Chan, K.L., Palmai-Pallag, T., Ying, S., and Hickson, I.D. (2009). Replication stress induces sister-chromatid bridging at fragile site loci in mitosis. Nat. Cell Biol. *11*, 753–760.

Christman, M.F., Dietrich, F.S., and Fink, G.R. (1988). Mitotic recombination in the rDNA of S. cerevisiae is suppressed by the combined action of DNA topoisomerases I and II. Cell *55*, 413–425.

Cuvier, O., Stanojcic, S., Lemaitre, J.M., and Mechali, M. (2008). A topoisomerase II-dependent mechanism for resetting replicons at the S-M-phase transition. Genes Dev. *22*, 860–865.

Dalgaard, J.Z., and Klar, A.J. (2000). swi1 and swi3 perform imprinting, pausing, and termination of DNA replication in S. pombe. Cell *102*, 745–751.

Dawlaty, M.M., Malureanu, L., Jeganathan, K.B., Kao, E., Sustmann, C., Tahk, S., Shuai, K., Grosschedl, R., and van Deursen, J.M. (2008). Resolution of sister centromeres requires RanBP2-mediated SUMOylation of topoisomerase IIalpha. Cell *133*, 103–115.

Deshpande, A.M., and Newlon, C.S. (1996). DNA replication fork pause sites dependent on transcription. Science *272*, 1030–1033.

DiNardo, S., Voelkel, K., and Sternglanz, R. (1984). DNA topoisomerase II mutant of Saccharomyces cerevisiae: topoisomerase II is required for segregation of daughter molecules at the termination of DNA replication. Proc. Natl. Acad. Sci. USA *81*, 2616–2620.

Doksani, Y., Bermejo, R., Fiorani, S., Haber, J.E., and Foiani, M. (2009). Replicon dynamics, dormant origin firing, and terminal fork integrity after double-strand break formation. Cell *137*, 247–258.

Duggin, I.G., Wake, R.G., Bell, S.D., and Hill, T.M. (2008). The replication fork trap and termination of chromosome replication. Mol. Microbiol. *70*, 1323–1333.

Edenberg, H.J., and Huberman, J.A. (1975). Eukaryotic chromosome replication. Annu. Rev. Genet. *9*, 245–284.

Fields-Berry, S.C., and DePamphilis, M.L. (1989). Sequences that promote formation of catenated intertwines during termination of DNA replication. Nucleic Acids Res. *17*, 3261–3273.

Greenfeder, S.A., and Newlon, C.S. (1992a). A replication map of a 61-kb circular derivative of Saccharomyces cerevisiae chromosome III. Mol. Biol. Cell *3*, 999–1013.

Greenfeder, S.A., and Newlon, C.S. (1992b). Replication forks pause at yeast centromeres. Mol. Cell. Biol. *12*, 4056–4066.

Gruber, M., Wellinger, R.E., and Sogo, J.M. (2000). Architecture of the replication fork stalled at the 3′ end of yeast ribosomal genes. Mol. Cell. Biol. *20*, 5777–5787.

Henikoff, S., Ahmad, K., and Malik, H.S. (2001). The centromere paradox: stable inheritance with rapidly evolving DNA. Science *293*, 1098–1102.

Hiasa, H., and Marians, K.J. (1994). Tus prevents overreplication of oriC plasmid DNA. J. Biol. Chem. *269*, 26959–26968.

Holm, C., Goto, T., Wang, J.C., and Botstein, D. (1985). DNA topoisomerase II is required at the time of mitosis in yeast. Cell *41*, 553–563.

Holm, C., Stearns, T., and Botstein, D. (1989). DNA topoisomerase II must act at mitosis to prevent nondisjunction and chromosome breakage. Mol. Cell. Biol. *9*, 159–168.

Ivessa, A.S., Lenzmeier, B.A., Bessler, J.B., Goudsouzian, L.K., Schnakenberg, S.L., and Zakian, V.A. (2003). The Saccharomyces cerevisiae helicase Rrm3p facilitates replication past nonhistone protein-DNA complexes. Mol. Cell *12*, 1525–1536.

Katou, Y., Kanoh, Y., Bando, M., Noguchi, H., Tanaka, H., Ashikari, T., Sugimoto, K., and Shirahige, K. (2003). S-phase checkpoint proteins Tof1 and Mrc1 form a stable replication-pausing complex. Nature *424*, 1078–1083.

Kobayashi, T. (2006). Strategies to maintain the stability of the ribosomal RNA gene repeats—collaboration of recombination, cohesion, and condensation. Genes Genet. Syst. *81*, 155–161.

Lambert, S., Watson, A., Sheedy, D.M., Martin, B., and Carr, A.M. (2005). Gross chromosomal rearrangements and elevated recombination at an inducible site-specific replication fork barrier. Cell *121*, 689–702.

Lemoine, F.J., Degtyareva, N.P., Lobachev, K., and Petes, T.D. (2005). Chromosomal translocations in yeast induced by low levels of DNA polymerase a model for chromosome fragile sites. Cell *120*, 587–598.

Lengronne, A., Pasero, P., Bensimon, A., and Schwob, E. (2001). Monitoring S phase progression globally and locally using BrdU incorporation in TK(+) yeast strains. Nucleic Acids Res. *29*, 1433–1442.

Liberi, G., Maffioletti, G., Lucca, C., Chiolo, I., Baryshnikova, A., Cotta-Ramusino, C., Lopes, M., Pellicioli, A., Haber, J.E., and Foiani, M. (2005). Rad51-dependent DNA structures accumulate at damaged replication forks in sgs1 mutants defective in the yeast ortholog of BLM RecQ helicase. Genes Dev. *19*, 339–350.

Lopes, M., Cotta-Ramusino, C., Liberi, G., and Foiani, M. (2003). Branch migrating sister chromatid junctions form at replication origins through Rad51/Rad52-independent mechanisms. Mol. Cell *12*, 1499–1510.

Lucas, I., Germe, T., Chevrier-Miller, M., and Hyrien, O. (2001). Topoisomerase II can unlink replicating DNA by precatenane removal. EMBO J. *20*, 6509–6519.

Lydall, D., and Whitehall, S. (2005). Chromatin and the DNA damage response. DNA Repair (Amst.) *4*, 1195–1207.

Mohanty, B.K., Bairwa, N.K., and Bastia, D. (2006). The Tof1p-Csm3p protein complex counteracts the Rrm3p helicase to control replication termination of Saccharomyces cerevisiae. Proc. Natl. Acad. Sci. USA *103*, 897–902.

Olavarrieta, L., Hernández, P., Krimer, D.B., and Schvartzman, J.B. (2002). DNA knotting caused by head-on collision of transcription and replication. J. Mol. Biol. *322*, 1–6.

Postow, L., Ullsperger, C., Keller, R.W., Bustamante, C., Vologodskii, A.V., and Cozzarelli, N.R. (2001). Positive torsional strain causes the formation of a four-way junction at replication forks. J. Biol. Chem. *276*, 2790–2796.

Raghuraman, M.K., Winzeler, E.A., Collingwood, D., Hunt, S., Wodicka, L., Conway, A., Lockhart, D.J., Davis, R.W., Brewer, B.J., and Fangman, W.L. (2001). Replication dynamics of the yeast genome. Science *294*, 115–121.

Schwacha, A., and Kleckner, N. (1994). Identification of joint molecules that form frequently between homologs but rarely between sister chromatids during yeast meiosis. Cell *76*, 51–63.

Sogo, J.M., Lopes, M., and Foiani, M. (2002). Fork reversal and ssDNA accumulation at stalled replication forks owing to checkpoint defects. Science *297*, 599–602.

Spell, R.M., and Holm, C. (1994). Nature and distribution of chromosomal intertwinings in Saccharomyces cerevisiae. Mol. Cell. Biol. *14*, 1465–1476.

Sundin, O., and Varshavsky, A. (1981). Arrest of segregation leads to accumulation of highly intertwined catenated dimers: dissection of the final stages of SV40 DNA replication. Cell *25*, 659–669.

Suski, C., and Marians, K.J. (2008). Resolution of converging replication forks by RecQ and topoisomerase III. Mol. Cell *30*, 779–789.

Tuduri, S., Crabbé, L., Conti, C., Tourrière, H., Holtgreve-Grez, H., Jauch, A., Pantesco, V., De Vos, J., Thomas, A., Theillet, C., et al. (2009). Topoisomerase I suppresses genomic instability by preventing interference between replication and transcription. Nat. Cell Biol. *11*, 1315–1324.

Vidanes, G.M., Bonilla, C.Y., and Toczyski, D.P. (2005). Complicated tails: histone modifications and the DNA damage response. Cell *121*, 973–976.

Wang, J.C. (2002). Cellular roles of DNA topoisomerases: a molecular perspective. Nat. Rev. Mol. Cell Biol. *3*, 430–440.

Wang, Y., Vujcic, M., and Kowalski, D. (2001). DNA replication forks pause at silent origins near the HML locus in budding yeast. Mol. Cell. Biol. *21*, 4938–4948.

Wang, X., Reyes-Lamothe, R., and Sherratt, D.J. (2008). Modulation of Escherichia coli sister chromosome cohesion by topoisomerase IV. Genes Dev. *22*, 2426–2433.

Yabuki, N., Terashima, H., and Kitada, K. (2002). Mapping of early firing origins on a replication profile of budding yeast. Genes Cells *7*, 781–789.

Zhu, J., Newlon, C.S., and Huberman, J.A. (1992). Localization of a DNA replication origin and termination zone on chromosome III of Saccharomyces cerevisiae. Mol. Cell. Biol. *12*, 4733–4741.